Phytochemistry Letters 30 (2019) 26–30

Contents lists available at ScienceDirect

Phytochemistry Letters

journal homepage: www.elsevier.com/locate/phytol

Ligand-based virtual screening and molecular docking of two cytotoxic compounds isolated from *Papaver lacerum*

Omer Bayazeid[a], Erdal Bedir[b], Funda N. Yalcin[a,*]

[a] Department of Pharmacognosy, Hacettepe University, Ankara, Turkey
[b] Department of Bioengineering, Faculty of Engineering, İzmir Institute of Technology, Urla, İzmir, Turkey

ARTICLE INFO

Keywords:
Papaver
Cytotoxicity
In silico
Molecular docking
Tyrosol-1-*O*-*β*-xylopyranosyl-(1→6)-*O*-*β*-glucopyranoside
5-*O*-(6-*O*-*α*-rhamnopyranosyl-*β*-glucopyranosyl) mevalonic acid

ABSTRACT

This study revealed that the *Papaver lacerum* extract strongly inhibited HeLa cell proliferation, resulting in 13% cell viability. As a result of phytochemical studies, one known compound, Tyrosol-1-*O*-*β*-xylopyranosyl-(1→6)-*O*-*β*-glucopyranoside) (**I**), and one new compound, 5-*O*-(6-*O*-*α*-rhamnopyronosyl-*β*-glucopyronosyl) mevalonic acid (**II**), were isolated. Compounds **I** and **II** were found to possess a moderate cytotoxic effect with an IC_{50} of 66.4 μM ($p < 0.0001$) and 54 μM ($p < 0.0001$), respectively. The ligand-based virtual screening technique was used to reveal the possible molecular target of compounds **I** and **II**. The molecular target was identified as protein-tyrosine kinase Syk for compound **I**, and aldo-keto reductase family-1 for compound **II**. Molecular docking was used to assess the binding affinity of the compounds with the targets obtained from ligand-based virtual screening.

1. Introduction

A total of 110 *Papaver* species are distributed around the world, of which 50 grow wildly in Turkey with ten being endemic species (Güner et al., 2000). *Papaver* genus, consisting of annual, biennial and perennial herbs, is native to habitats throughout East Europe, Middle East, US, and Turkey (Davis, 1972; Sarıyar et al., 2002). *Papaver* species have been used to treat a variety of diseases, including inflammation, sleep disorders, cough, and analgesia (Kostic et al., 2010). Previous studies using brine shrimp assays revealed that methanolic extracts of *P. pavoninum* and *P. dubium* exhibited a cytotoxic effect (Ibrar et al., 2015; Mat et al., 2000). Furthermore, the *P. somniferum* extract showed strong anti-proliferative activity against the HeLa and HT29 cell lines (Güler et al., 2016) whereas *P. rhoeas* had an anticancer effect on the MCF7 and HCT116 cell lines (Hijazi et al., 2017). In this study, five *Papaver* species were collected and screened to determine their anticancer activity on the HeLa cell line. The most active species was selected for further phytochemical analysis. Due to the extensive studies on the alkaloids content in *Papaver* species (Sarıyar et al., 2002), non-alkaloidal fractions were chosen for chemical isolation. Two secondary metabolites were isolated, and their structures were identified by spectroscopic methods. The cytotoxicity of the extracts and the isolated compounds were evaluated by MTT assay. The possible molecular targets of the isolated compounds were established through ligand-based virtual screening and molecular docking.

2. Results and discussion

The MeOH extracts were obtained from the aerial parts of *P. macrostomum*, *P. syriacum, P. glaucum*, *P. rhoeas,* and *P. lacerum* by maceration. The methanolic extracts were used for the cytotoxicity tests. The cytotoxicity effects of the *Papaver* extracts are demonstrated in Fig. 1. *P. lacerum* (100 μg/mL) was the most cytotoxic extract with 13% cell viability ($p < 0.0001$). The phytochemical analysis of the *P. lacerum* extract resulted in the isolation of compounds **I** and **II**.

Compound **I** was isolated as a colorless amorphous powder. LC/ESI-MS exhibited an $[M+Na]^+$ ion at *m/z* 455, suggesting the molecular formula of $C_{19}H_{28}O_{11}$, 432. The ^{1}H-NMR signals revealed that compound **I** had a para-substituted aromatic ring [δ_H 7.09 (2H, d, $J = 8.5$ Hz, H-3 and 5), 6.94 (2H, d, $J = 8.5$ Hz, H-2 and 6)], and aliphatic protons [δ_H 2.64 (2H, t, $J = 7.0$ Hz, H-7) and 3.52 (2H, t, $J = 6.7$ Hz, H-8)] in the aglycon part, which was almost identical with the spectral data of tyrosol (Rasser et al., 2000). This assumption was further supported by the ^{13}C-NMR resonances at δ 156.17 (C-1), 133.13

Abbreviations: AKR1C3, aldo-keto reductase family 1-member C 3; $CHCl_3$, chloroform; DMEM, Dulbecco's modified Eagle's medium; EtOAc, ethyl acetate; FBS, fetal bovine serum; HR-ESI-MS, high-resolution electrospray ionization mass spectrometry; MeOH, methanol; MOE, molecular operating environment; MTT, MTT (3-(4,5-dimethylthiazol-2- yl)-2,5- Diphenyltetrazolium Bromide); ROCS, rapid overlay of chemical structures

* Corresponding author at: Hacettepe University, Faculty of Pharmacy, Department of Pharmacognosy, 06100, Ankara, Turkey.
E-mail address: funyal@hacettepe.edu.tr (F.N. Yalcin).

https://doi.org/10.1016/j.phytol.2019.01.007
Received 17 October 2018; Received in revised form 31 December 2018; Accepted 7 January 2019
Available online 11 January 2019

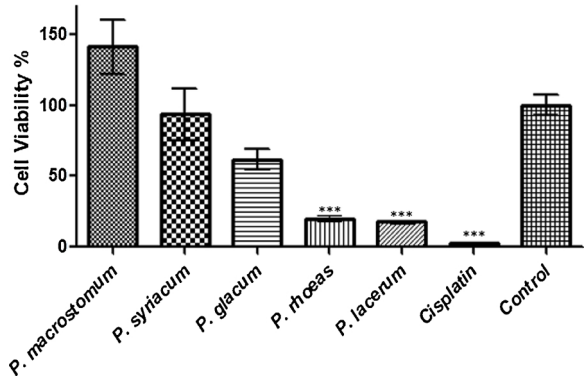

Fig. 1. Cytotoxicity of the Papaver extracts (100 µg/mL) on the HeLa cells. Cisplatin at 30 µM, *** ($p < 0.0001$).

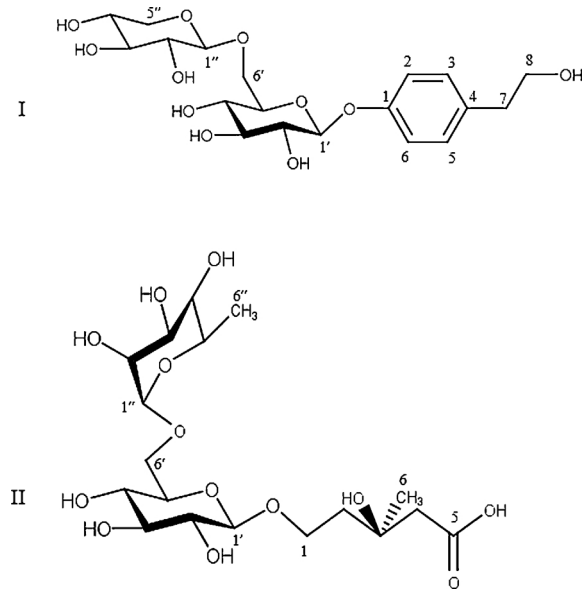

Fig. 2. Structure of compounds **I** and **II**.

(C-4), 130.12 (C-3 and C-5), and 116.56 (C-2 and C-6), 38.67 (C-7), and 62.8 (C-8). On the other hand, the ^{1}H spectrum demonstrated the presence of two anomeric protons at the lower field, attributed to two *β*-sugar moieties [δ_H 4.71 (1H, d, $J = 7.2$ Hz, H-1′) and 4.16 (1H, d, $J = 7.4$ Hz, H-1″)] whereas anomeric carbons were observed at δ_C 101.12 (C-1′) and δ_C 104.27 (C-1″) in the carbon spectrum. Based on the spectral data of compound **I**, which was also assigned fully by inspecting the 2D NMR spectra, the correlation between H-1″ and C 6′ (δ 68.81) confirmed that *β*-xylopyranose was connected to the *β*-glucopyranose at the C 6′ position. Additionally, in the HMBC spectrum, the correlation between H-1′ and C-1 (δ 156.17) suggested that *β*-glucopyranose was connected to the A2B2 ring. Likewise, H-2 correlated to C 6 (δ 116.56), and H-4 correlated to C 5 (δ 130.12). Thus, the structure of compound **I** was concluded to be identical with tyrosol-1-*O*-*β*-xylopyranosyl-(1→6)-*O*-*β*- glucopyranoside (Fig. 2) (Sawasdee et al., 2010).

Compound **II** was isolated as a yellowish amorphous powder, which gave a molecular formula of $C_{18}H_{33}O_{13}$, determined by HR-MS-Q-TOF at the $[M-H]^-$ ion peak at *m/z* 455.1859 (calc. for $C_{18}H_{33}O_{13}$, 456.1848). The ^{1}H-NMR spectrum displayed two anomeric protons at δ_H 4.02 (d, $J = 7.6$ Hz, H-1') and δ_H 4.56 (d, $J = 1.0$ Hz, H-1"). The two anomeric protons correlated to the carbons at δ 103.8 (C-1′) and 101.8 (C-1″), respectively, which were later attributed to *β*-glucose and *α*-rhamnose residues by further examining the 1- and 2D NMR spectra (Table 1). Besides the sugar resonances, the ^{13}C-NMR and HSQC spectra revealed the presence of one methyl, three methylene and two

Table 1
Compound II (MRG) in the ^{1}H-NMR and ^{13}C- NMR spectra (DMSO-d_6, ^{1}H: 400 MHz, ^{13}C: 100 MHz) (δ in ppm, J in Hz).

No.	Carbon type	δ_C	δ_H / J
Aglycon			
1_a	CH_2	66.5	3.79 (1H, d, $J = 9.94$)
1_b			3.40 (1H, m)
2_a	CH_2	42.2	1.63 (1H, m)
2_b			1.53 (1H, m)
3	C	69.46	–
4_a	CH_2	47.3	2.07 (1H, d, $J = 14.78$)
4_b			1.90 (1H, d, $J = 14.79$)
5	C	177.9	–
6	CH_3	29.1	1.01 (3H, s)
Glucose			
1'	CH	103.8	4.02 (1H, d, $J = 7.64$)
2'	CH	73.8	2.89 (1H, m)
3'	CH	76.7	3.13 (1H, m)
4'	CH	70.78	3.42 (1H, m)
5'	CH	75.8	3.21 (1H, m)
$6'_a$	CH_2	67.8	3.79 (1H, d, $J = 9.94$)
$6'_b$			3.38 (1H, m)
Rhamnose			
1”	CH	101.8	4.56 (1H, d $J = 1.01$)
2”	CH	69.6	3.62 (1H, dd, $J = 1.44/3.11$)
3”	CH	68.9	3.42 (1H, m)
4”	CH	72.5	3.13 (1H, m)
5”	CH	70.96	2.92 (1H, m)
6”	CH_3	17.9	1.11 (3H, d, $J = 6.29$)

quaternary carbons, one of which suggested a carboxylic acid carbonyl at δ_C 177.9 and an additional oxygenated carbon at δ_C 69.46. A detailed analysis of the COSY, HSQC and HMBC spectra and the comparison of the spectral data with those reported in the literature allowed identifying the aglycone part as mevalonic acid, a key intermediate of terpenoid biosynthesis. Furthermore, the down-shielded methyl carbon at δ_C 29.1 showed a strong HMBC correlation to the oxygenated carbon at δ_C 69.46, implying their nearness. The downfield shifting of the methylene carbon assigned to C-1 (δ_C 66.5), and the HMBC correlation between the anomeric proton of glucose and C-1 indicated the position of the glycosidic linkage as C-1(*O*). In addition, the HMBC spectrum revealed a correlation between C-6′ and H-1″ (δ 67.8), suggesting that rhamnose was connected to glucose. Therefore, the structure of compound **II** was determined as 5-*O*-(6-*O*-*α*-rhamnopyranosyl-*β*-glucopyranosyl) mevalonic acid, which is a new compound (Fig. 2).

Compounds **I** and **II** were evaluated for their cytotoxic effects on the HeLa cell line using an MTT cytotoxicity assay. Compound **I** was cytotoxic to HeLa cells with an IC_{50} of 66.4 µM ($p < 0.0001$) (Fig. 3), while compound **II** was cytotoxic with an IC_{50} of 54 µM ($p < 0.0001$) (Fig. 3). Cisplatin 30 µM was used as a positive control. In addition, neither compound (100 µM) showed any cytotoxic effect on the normal cell line L929. Similarly, the *P. lacerum* MeOH extract and the two compounds inhibited the colony formation of the HeLa cells compared

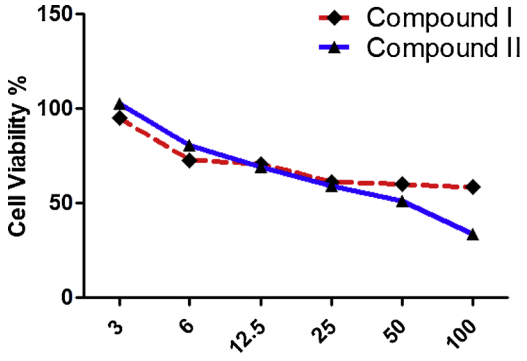

Fig. 3. Cytotoxic effect of compounds **I** and **II**.

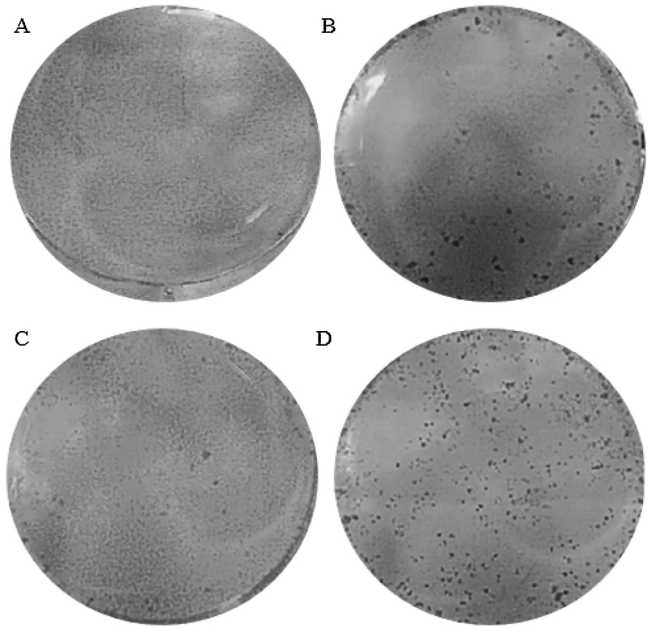

Fig. 4. Colony formation assay A. *P. lacerum* extract, B. Compound **I**, C. Compound **II**, D. Control. Colonies are shown in black dots.

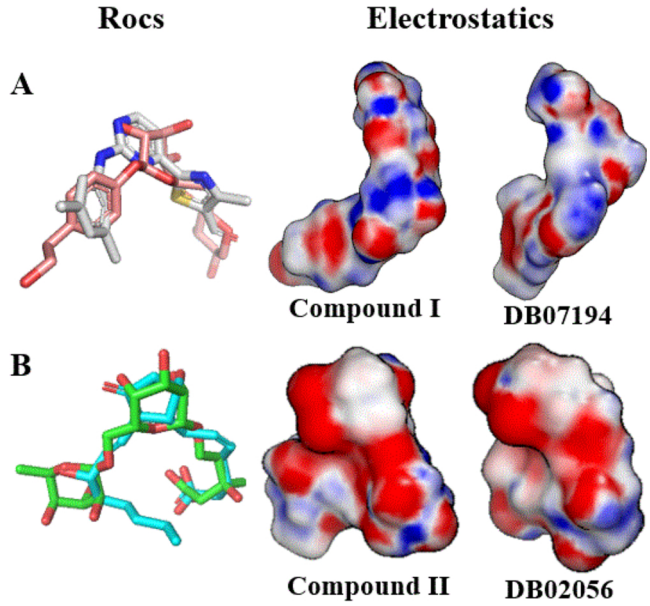

Fig. 5. Rocs: (A) Overlay of compound **I** (pink) and DB07194 (gray), (B) Overlay of compound **II** (green) and DB02056 (blue). Electrostatics: Electrostatics map of compounds **I** and **II** compared with their similar compounds (electrostatic surfaces: blue for positive and red for negative) (For interpretation of the references to colour in this figure legend, the reader is referred to the web version of this article).

to the control (Fig. 4).

The 3D similarities of compounds **I** and **II** were compared against known ligands using ligand-based virtual screening methods ROCs and EON. According to the fragment-hopping strategy used in previous studies, compounds with top-ranking scores higher than 0.62 for the electrostatic Tanimoto (ET) and 0.75 and higher for *TanimotoCombo* were chosen for the visual analysis. Therefore, we examined the area with the highest values for 3D similarity to reference compounds **I** and **II** (Saluste et al., 2012). Analyzing compound **I,** the 3D similarity results led to the selection of a similar ligand with Drugbank **ID: DB07194**, which targets tyrosine-protein kinase SKY (Law et al., 2014). The TanimotoCombo score was 0.80, and the ET-Combo score was 0.937 (Fig. 5-A). Protein-tyrosine kinase Syk expression is known to inhibit cell motility by improving cell-cell contacts. The hypothesis is that protein-tyrosine kinase Syk acts as a tumor suppressor and has an effect through cell adhesion and motility (Zhang et al., 2009). On the other hand, evaluation of the 3D similarity of compound **II** resulted in selecting a ligand with Drugbank **ID: DB02056**, which targets aldo-keto reductase family 1-member C (AKR1C3). (Law et al., 2014). The TanimotoCombo score was 0.832, and the ET-Combo score was 1.38 (Fig. 5-B). A previous study showed that the AKR1C3 gene might be associated with drug resistance, such as the chemotherapy drug cisplatin. It was also reported that overexpression of AKR1C3 was narrowly associated with anti-cancer medications resistance. Mefenamic acid, an AKR1C3 enzyme inhibitor, increased the sensitivity of anticancer drugs (Shiiba et al., 2017).

Compounds **I** and **II** were successfully docked in the inhibitor binding pockets of **4RSS** and **3UG8**, respectively. In the binding pocket, hydrogen-bonding and hydrophobic interactions with amino acids were observed for both compounds. Molecular docking was completed via the molecular operating environment (MOE.2014) for compounds **I**, **II** on tyrosine-protein kinase SYK (**4RSS**.pdb) and AKR1C3 (**3UG8**.pdb), respectively with the scoring affinity London dG and GBVI/WSA dG. The docking score for compound **I** in the binding pockets of **4RSS** is -6.536 and **RMSD** = 1.357 kcal/mol. The amino acids involved in the binding mode between tyrosine-protein kinase SKY and its inhibitor pyrazolylpyrimidines are **Asp-512**, **Arg-498**, **Gly-454**, **Leu-377**, **Pro-455**, **Leu-501**, and **Ala-451** (Choi et al., 2015). Visualization the interaction in the binding pocket, the phenolic OH of carbon 3, 4 in compound **I** acted as an H-bond donor with **Asp-512**, while the benzene ring formed an arene-H bond with **Pro-455** and **Leu-377** (Fig. 6-A). The docking score for compound **II** in the binding pockets of **3UG8** is -6.550 and **RMSD** = 1.636 kcal/mol. The amino acids involved in the binding site between AKR1C3 and its inhibitor indomethacin are **Try-55**, **Trp-227**, **Met-120**, **Phe-306**, and **Phe-306** (Flanagan et al., 2012). Visualization the interaction in the binding site, compound **II** formed an arene-H bond between xylose and **Phe-306**, and the OH group in carbon 2 of glucose acted as an H-bond acceptor (Fig. 6-B). In brief, the binding mode of compounds **I** and **II** in the binding site of **4RSS** and **3UG8**, respectively suggested that the former might act through the inhibition of tyrosine-protein kinase SKY and the latter might act as an AKR1C3 inhibitor.

In conclusion, two compounds were isolated from the aqueous extract of *P. lacerum*. Compound **I** was previously isolated from *Miliusa mollis*, and this is the second report of its existence in nature. Compound **II** was identified as a mevalonic acid derivative. Mevalonic acid is a key precursor of many terpenic metabolites biosynthesis in the plant kingdom. Both compounds exhibited a moderate antineoplastic effect on the HeLa cell line without any noteworthy effect on the normal cell line L929. Their possible molecular targets were identified through ligand-based virtual screening and molecular docking, revealing that compound **I** might act through the inhibition of tyrosine-protein kinase SKY and compound **II** might act as an AKR1C3 inhibitor.

3. Experimental

3.1. General

For the cell culture, Cisplatin, DMEM (Biochrom, Germany), penicillin/Streptomycin (Wisent, Canada), L- Glutamine (Lonza, Belgium), FBS (Biowest, USA), trypsin EDTA (Lonza, Belgium), and PBS tablets (Biomatik, Canada) were used. The color difference in the MTT assay was detected by a spectrophotometer (BioTek-uquant 193379). The materials used for phytochemical analysis were n-hexane (Sigma, Merck), DMSO (Sigma, USA), methanol (Sigma, Merck), chloroform (Sigma, Merck), ethyl acetate (Sigma, Merck), dichloromethane (Sigma, Merck), n-butanol (Merck), t-butanol (Sigma, Merck), ethanol (Sigma,

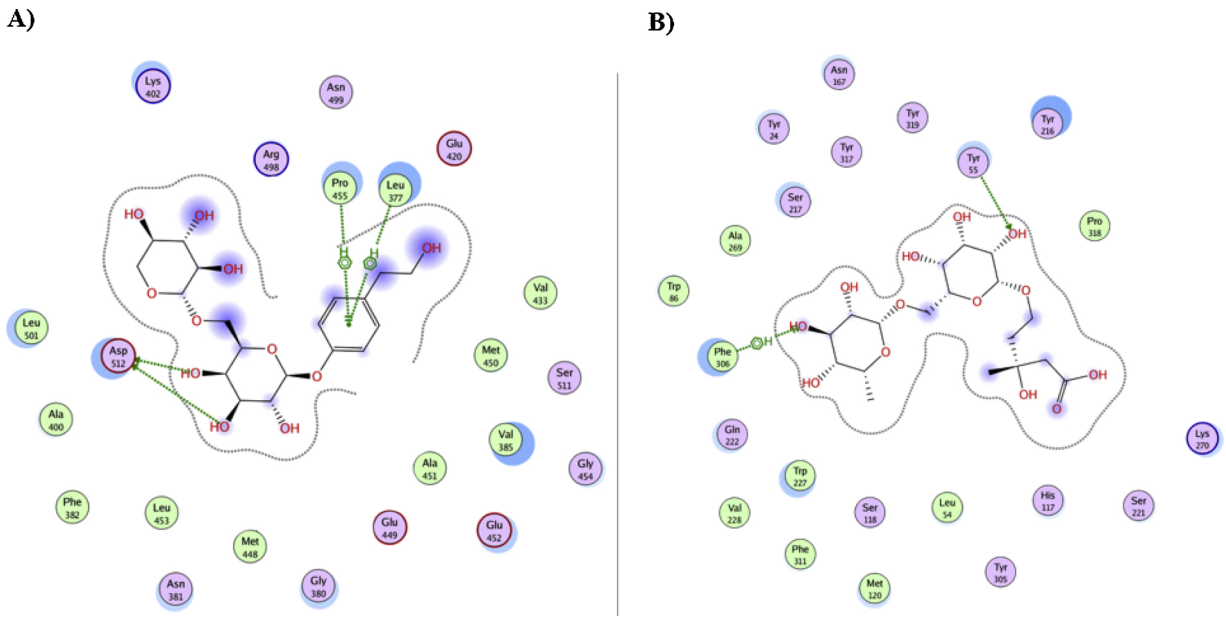

Fig. 6. 2D ligand interaction in the binding site: A) Compound **I** in complex with tyrosine protein kinase SYK. B) Compound **II** in complex with AKR1C3.

Merck), and acetic acid (Merck). The results of nuclear magnetic resonance were obtained using the MERCURY plus-AS 400 system. A Mass LC/ESI-MS spectrometer (Shimadzu LCMS-8030 triple quadrupole) was utilized for normal resolution and Mass Q-TOF LC/MS (Agilent 6530) for high resolution.

3.2. Plant material

The aerial parts of the *Papaver* species were collected from the eastern and middle regions of Anatolia in May 2014 during the flowering period. The species were identified by Prof. Dr. Galip Akaydın, Department of Plant Biology, Hacettepe University (Ankara, Turkey), where the herbarium samples were deposited as *P. rhoeas* (16019-HEF), *P. lacerum* (16020-HEF), *P. syriacum* (16021-HEF), and *P. macrostomum* (16022-HEF) *P. glaucum* (16023-HEF)].

3.3. Extraction and isolation

The aerial parts of the *Papaver* species were dried in shade and powdered. The MeOH extracts were obtained by maceration of plant material with 1000 mL X 3 of MeOH for three days at room temperature. The extract was filtered and dried under reduced pressure at 40 °C (Yields: *P. glaucum*: 12.0%, *P. macrostomum*: 11.3%, *P. rhoeas*: 6.8%, *P. lacerum*: 6.4%, and *P. syriacum*: 7.0%). The same extraction procedure was used for the biological activity tests. The dried *P. lacerum* extract (145 g) was dissolved in 250 mL of water and extracted with 250 mL × 3 of EtOAc.

1The H_2O soluble extract (8.7 g) was separated by C-18 VLC (5 × 40 cm), eluting with 100% water (H_2O) with decreasing polarity (10% MeOH → 100% MeOH), LH-20 Sephadex column (LH-20) (2.5 × 30 cm), eluting with CH_2Cl_2-MeOH (50:50) and silica gel column (3 × 40 cm), eluting with $CHCl_3$-MeOH-H_2O (90:10:1→ 70:30:3 and 100% MeOH) to produce Fractions 1-5.

Fraction 4 was subjected to C-18 VLC (2 × 10 cm), eluting with 100% H_2O with decreasing polarity (10% MeOH → 100% MeOH) and purified by an LH-20 Sephadex column (LH-20) (2.5 × 30 cm), eluting with CH_2Cl_2-MeOH (50:50) (Compound **I**: 3.5 mg).

Fraction 2 was subjected to a C-18 VLC (2 × 10 cm), eluting with (100% H_2O → 100% MeOH). Three fractions were collected including a fraction with the pure compound (11.7 mg) (Compound **II**).

3.4. Ligand-based virtual screening

Ligand-based virtual screening has been extensively applied in the recent years to identify specific chemical probes. It is a technique that can compare a library of chemical compounds with a ligand that is known for its activity and has the advantages of being fast and effective, and not requiring knowledge of the 3D structure of the target protein/receptor (Shin et al., 2015). In this study, our aim was to identify the possible mechanism of action of two cytotoxic compounds isolated from *P. lacerum.* In this study, we used ligand-based virtual screening to identify the relevant chemical structure across the DrugBank library (Wishart et al., 2006) using Rocs and EON, OpenEye programs [https://www.eyesopen.com] (Swann et al., 2011; López-Ramos and Perruccio, 2010). The test protocol was used as illustrated by (Rahman and Rahman, 2017) with slight modifications.

3.5. MTT cytotoxicity test

To evaluate the cytotoxicity of the *Papaver* extracts and compounds **I** and **II** obtained from the *P. lacerum* extract, we ran an MTT cell cytotoxicity assay. The HeLa cells were cultured in a T-25 flask in DMEM with supplements at 37 °C with 5% CO_2. The cells were transferred into a T-75 flask after the confluence reached 80%. The cells were seeded in 96 well-plated for 24 h at 37 °C at a density of 1×10^4 cells per well. After 24 h, they were treated with extracts/compounds/drugs in a free serum medium containing 100 µL/well and incubated for 48 h. The commercial cisplatin was used as a positive control. After 48 h, 10 µL of MTT solution (25 mg/mL) was added to each well and incubated for 4 h at 37 °C. After incubation, the cell supernatants were removed and 100 µL of DMSO was added and incubated for 10 min. The color was measured with a 96-well plate reader at 450 nm. In this experiment, three different batches of cells were used (n = 3) (Du et al., 2017).

3.6. Colony formation assay

10^3 HeLa cells were seeded into each well in six-well plates, each sample in triplicate. After nine days, when the cells formed colonies, they were fixed with (70:30 MeOH: Acetic acid) for half an hour on the workbench. After fixation, MeOH:acetic acid solution was removed from each well, and 1 mL of 0.2% crystal violet (v/v in water) was added into each well. Seventy-five plates were left to stain for half an

hour on the workbench. The excess stain was removed and the wells were washed with milliQ water to eliminate non-specific staining. The wells were left to dry on the workbench, and then the colonies were counted (Franken et al., 2006).

3.7. Molecular docking

The 3D structures of tyrosine-protein kinase SYK (PDB code: 4RSS) in complex with pyrazolylpyrimidines (Choi et al., 2015) and AKR1C3 (PDB code: 3UG8) in complex with indomethacin (Flanagan et al., 2012) were downloaded from the Protein Data Bank (www.rcsb.org). Molecular docking was performed using MOE program (2014.09). Hydrogen atoms and partial charges were added to the protein. Protein minimization was performed with the side chains kept rigid and the ligand flexible. The selected site was isolated and minimized followed by protonating the protein. The 3D ligands were minimized using MMFF94x with the cutoffs of 10 Å to 12 Å. The hydrogens and charges were fixed, and the RMS gradient was set to 0.001 kcal/mol (El-Nakkady et al., 2012).

3.8. Statistical analysis

The results were presented as mean ± SEM (n = 3). The differences between the groups were compared using one-way analysis of variance (One-way ANOVA and nonparametric), followed by the Tukey test for multiple comparisons using GraphPad Prism 5 program, and p values of 0.05 or less were regarded as significant.

Conflict of interest

The authors declare that there are no conflicts of interest.

Acknowledgments

This study was financially supported by TÜBİTAK Ph.D. fellowship (2215) and Hacettepe University Scientific Researches Coordination Unit (Project Number: 014 D11 301 003-734). The author would like to thank OpenEye scientific for providing free academic licenses of their software packages.

Appendix A. Supplementary data

Supplementary material related to this article can be found, in the online version, at doi:https://doi.org/10.1016/j.phytol.2019.01.007.

References

Choi, J.S., Hwang, H.J., Kim, S.W., Lee, B.I., Lee, J., Song, H.J., Koh, J.S., Kim, J.H., Lee, P.H., 2015. Highly potent and selective pyrazolylpyrimidines as Syk kinase inhibitors. Bioorg. Med. Chem. Lett. 25, 4441–4446. https://doi.org/10.1016/j.bmcl.2015.09.011.

Davis, P.H., 1972. Flora of Turkey and East Aegean Islands, second ed. University Press, Edinburgh, Edinburgh.

Du, Y., Zhang, W., He, R., Ismail, M., Ling, L., Yao, C., Fu, Z., Li, X., 2017. Dual 7-ethyl-10-hydroxycamptothecin conjugated phospholipid prodrug assembled liposomes with *in vitro* anticancer effects. Bioorg. Med. Chem. Lett. 25, 3247–3258. https://doi.org/10.1016/j.bmc.2017.04.025.

El-Nakkady, S.S., Hanna, M.M., Roaiah, H.M., Ghannam, I.A., 2012. Synthesis, molecular docking study and antitumor activity of novel 2-phenylindole derivatives. EJMC 47, 387–398. https://doi.org/10.1016/j.ejmech.2011.11.007.

Flanagan, J.U., Yosaatmadja, Y., Teague, R.M., Chai, M.Z., Turnbull, A.P., Squire, C.J., 2012. Crystal structures of three classes of non-steroidal anti-inflammatory drugs in complex with aldo-keto reductase 1C3. PLoS One 7, e43965. https://doi.org/10.1371/journal.pone.0043965.

Franken, N.A., Rodermond, H.M., Stap, J., Haveman, J., Van Bree, C., 2006. Clonogenic assay of cells in vitro. Nat. Protoc. 1, 2315–2319. https://doi.org/10.1038/nprot.2006.339.

Güler, D.A., Aydin, A., Koyuncu, M., Parmaksiz, I., 2016. Anticancer activity of *Papaver Somniferum*. JOTCSA 3, 349–366. https://doi.org/10.18596/jotcsa.43273.

Güner, A., Özhatay, N., Ekim, T., Başer, K.H.C., 2000. Flora of Turkey and the East Aegean Islands. Second Supplement, Edinburgh.

Hijazi, M.A., Aboul-Ela, M., Bouhadir, K., Fatfat, M., Khalife, H., Ellakany, A., Gali-Muhtasib, H., 2017. Cytotoxic activity of alkaloids from *Papaver rhoeas* growing in Lebanon. Rec. Nat. Prod. 11, 211.

Ibrar, M., Ehsan, M., Ullah, Barkat, Marwat, K.B., Mubarak, S.S., 2015. Cytotoxic and analgesic potentials of *Papaver pavoninum* Fisch & Mey. Pak. J. Bot. 47, 1895–1899.

Kostic, D.A., Mitic, S.S., Mitic, M.N., Zarubica, A.R., Velickovic, J.M., Dordevic, A.S., Randelovic, S.S., 2010. Phenolic contents, antioxidant and antimicrobial activity of *Papaver rhoeas* L. extracts from Southeast Serbia. JMPR 4, 1727–1732. https://doi.org/10.5897/JMPR10.121.

Law, V., Knox, C., Djoumbou, Y., Jewison, T., Guo, A.C., Liu, Y., Maciejewski, A., Arndt, D., Wilson, M., Neveu, V., Tang, A., Gabriel, G., Ly, C., Adamjee, S., Dame, Z.T., Han, B., Zhou, Y., Wishart, D.S., 2014. DrugBank 4.0: shedding new light on drug metabolism. NAR 42, 1091–1097. https://doi.org/10.1093/nar/gkt1068.

López-Ramos, M., Perruccio, F., 2010. HPPD: ligand-and target-based virtual screening on a herbicide target. J. Chem. Inf. Model. 50, 801–814. https://doi.org/10.1021/ci900498n.

Mat, A., Sariyar, G., Unsal, Ç., Deliorman, A., Atay, M., Özhatay, N., 2000. Alkaloids and bioactivity of *Papaver dubium* subsp. *dubium* and *P. dubium* subsp. *Laevigatum*. Nat. Prod. Lett. 14, 205–210. https://doi.org/10.1080/10575630008041232.

Rahman, S., Rahman, T., 2017. Unveiling some FDA-approved drugs as inhibitors of the store-operated Ca^{2+} entry pathway. Sci. Rep. 7, 12881. https://doi.org/10.1038/s41598-017-13343-x.

Rasser, F., Anke, T., Sterner, O., 2000. Secondary metabolites from a Gloeophyllum species. Phytochemistry 54, 511–516. https://doi.org/10.1016/S0031-9422(00)00137-0.

Saluste, G., Albarran, M.I., Alvarez, R.M., Rabal, O., Ortega, M.A., Blanco, C., Kurz, G., Salgado, A., Pevarello, P., Bischoff, J.R., Pastor, J., 2012. Fragment-hopping-based discovery of a novel chemical series of proto-oncogene PIM-1 kinase inhibitors. PLoS One 7, e45964. https://doi.org/10.1371/journal.pone.0045964.

Sarıyar, G., Mat, A., Ünsal, Ç., Özhatay, N., 2002. Biodiversity in the alkaloids of annual *Papaver* species of Turkish origin. Acta Pharm. Sci. 44, 159–164.

Sawasdee, K., Chaowasku, T., Likhitwitayawuid, K., 2010. New neolignans and a phenylpropanoid glycoside from twigs of *Miliusa mollis*. Molecules 15, 639–648. https://doi.org/10.3390/molecules15020639.

Shiiba, M., Yamagami, H., Yamamoto, A., Minakawa, Y., Okamoto, A., Kasamatsu, A., Sakamoto, Y., Uzawa, K., Takiguchi, Y., Tanzawa, H., 2017. Mefenamic acid enhances anticancer drug sensitivity via inhibition of aldo-keto reductase 1C enzyme activity. Oncol. Rep. 37, 2025–2032. https://doi.org/10.3892/or.2017.5480.

Shin, W.H., Zhu, X., Bures, M.G., Kihara, D., 2015. Three-dimensional compound comparison methods and their application in drug discovery. Molecules 20, 12841–12862. https://doi.org/10.3390/molecules200712841.

Swann, S.L., Brown, S.P., Muchmore, S.W., Patel, H., Merta, P., Locklear, J., Hajduk, P.J., 2011. A unified, probabilistic framework for structure-and ligand-based virtual screening. J. Med. Chem. 54, 1223–1232. https://doi.org/10.1021/jm1013677.

Wishart, D.S., Knox, C., Guo, A.C., Shrivastava, S., Hassanali, M., Stothard, P., Chang, Z., Woolsey, J., 2006. DrugBank: a comprehensive resource for *in silico* drug discovery and exploration. NAR 34, 668–672. https://doi.org/10.1093/nar/gkj067.

Zhang, X., Shrikhande, U., Alicie, B.M., Zhou, Q., Geahlen, R.L., 2009. Role of the protein tyrosine kinase Syk in regulating cell-cell adhesion and motility in breast cancer cells. Mol. Cancer Res. 7, 634–644. https://doi.org/10.1158/1541-7786.MCR-08-0371.